CIT/CoA/R-8710

Cranfield

CoA Report No 8710
July, 1987

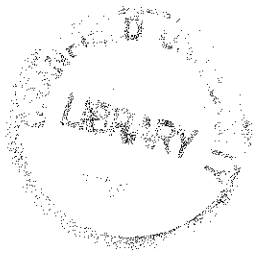

Compressible Flow Produced by Distributed Sources of Mass: An Exact Solution

J F Clarke

Aerodynamics, Cranfield Institute of Technology,
Cranfield, Bedford, MK43 0AL

Cranfield

CoA Report No 8710
July, 1987

Compressible Flow Produced by Distributed Sources of Mass: An Exact Solution

J F Clarke

Aerodynamics, Cranfield Institute of Technology,
Cranfield, Bedford, MK43 0AL

"The views expressed herein are those of the author alone and do not necessarily represent those of the Institute".

Abstract

The paper considers the case of a one-dimensional isentropic unsteady compressible flow that is driven entirely by a distribution of sources in the left-hand half space of an unbounded domain. The right-hand half-space contains no sources, so that source-strength drops discontinuously to zero as one crosses from left to right-hand space. Exact solutions are obtained for those parts of the flow that remain isentropic. A shock forms and grows at the right-hand head of the disturbances; the extent of the non-isentropic field that it creates is established, and is shown not to interfere with some novel developments that occur, some time after shock-formation, at the spatial point at which source-flow ceases. On a distance-time graph the left-going characteristics bifurcate at a cusp-locus on the time axis through the point of discontinuity in the source strength for all times after a critical value (provided that the source efflux is maintained). In physical terms the cusp-locus corresponds to a line of locally sonic flow, so that the source-provoked flow from left to right appears to 'choke' at this point. From this location onwards a segment of locally supersonic flow travels into the space to the right of the sources.

The problem has a number of interesting features, all of which can be analysed and exactly quantified. Consequently it provides a useful testing ground for numerical-solution algorithms, especially for situations in which source terms are present.

The problem is usefully illustrative of the sort of transient wave systems and flows that are generated by local massive gasification, or the ignition of a high-explosive charge, within a long pipe.

1. Introduction

An effective method of generating, rapidly, large amounts of gas for a variety of purposes is to burn a solid-propellant or high-explosive substance. This material is often provided in the form of bundles of grooved sticks of explosive, and the propellants in solid rocket motors are usually made up in the shape of hollow cylinders. When only a part of the whole length of the propellant burns, gas is created that begins to flow along the interstices or holes and there is an evident need to know how such flows develop from the very moment of their initiation. A similar state of affairs arises if a small high-explosive charge is ignited inside a pipe. The locally-generated pressures can be exploited in order to join together two (appropriately shaped) very long pipes, and it is clearly important to be able to predict these local values, as well as such things as shock-wave strengths in regions of the pipe far from the explosive charge. The overall situation within a gun barrel and breech can also be included in this broad category of configurations. The complete high-explosive charge acts as a source of high-pressure gas to propel the shot down the barrel of the gun. Transient pressure waves are generated during the early phases of propellant ignition and continue to interact with the burning material as the shot moves and burning continues.

To model such complex situations completely requires a study of the behaviour of the solid explosive itself, coupled with that of the chemically-reacting gases in which the propellant is bathed. This requires consideration of the full set of three-dimensional unsteady, multicomponent, reacting-gas Navier-Stokes equations. Even supposing that one could solve these equations, there is clearly every motivation to look for simpler models, that isolate key elements in the processes, and illuminate important physical features.

Since the examples described above all involve flows in long slender domains the simplification to a one-dimensional unsteady configuration is an obvious first step to take. A second simplifying step is to represent the generation of gas, that is solely responsible for the ensuing flow, by the use of source terms in the Euler equations of mass, momentum and energy conservation. Such terms are in the form of known functions of local gas properties, in general, and circumvent the complexities of chemical reactions, phase changes and so on. Such rationalisations are still widely used today in studies of internal ballistics (see, for example, Krier and Summerfield (1979)). It is

fair to say that numerical solutions of even the homogeneous forms of these equations are still not without their difficulties, as described by Roe (1986).

The development of computer codes for solution of the Euler equations is greatly assisted by the existence of exact analytical solutions for a few pertinent, perhaps idealised, configurations. Some current research on problems that involve source terms, as described above, has highlighted the absence of any exact solutions of these augmented Euler equations, and has stimulated the exercise whose results are reported here.

A problem that has the attributes of test-case and epitomiser of physical events is described in the present paper. A one-dimensional unsteady compressible flow of an ideal inviscid gas is assumed to contain a known distribution of sources in the left-hand half plane of an otherwise unbounded space; flow in the right-hand half plane is conventionally source-free. The actual character of the source distribution is chosen with an intention to ease the analysis but, despite this, remains acceptable from a physical point of view. Some brief general observations about conservation equations and source terms are made in Section 2, which also identifies the particular form of source terms that make analytical solutions possible. Section 3 adopts the hypothesis of isentropic flow and provides formal general solutions under this proviso. Section 3 also introduces the final postulate about the source terms, in the light of which it becomes a trivial matter to evaluate the integrals that appear in the formal general solution.

Explicit analytical solutions are written down in Section 4, and these begin to reveal details of the evolving flow field. Several features stand out at this stage, but two deserve special mention. The source-filled part of the field is dominated by rapidly-rising pressure, that is spatially uniform until a signal arrives that emanates from the point of discontinuous fall to zero in the source strength. To the right of this, the pressure falls as one moves further to the right and continues to do so until one crosses into the source-free regions. Clearly there is an expansion wave propagating into the source-filled regions from the low (and fixed) pressure domains on the right of the field; a compression wave travels from left to right into the low-pressure areas, and this initially continuous isentropic compression steepens to form a shock-wave at its head. This not unexpected feature is the first of the two mentioned above. The matter and some of its consequences is discussed in Section 5.

The second feature is novel, and owes its existence to the hypothesised discontinuous drop in source strength between left and right-hand half planes. Characteristics lines of the left-going family on a distance-time plot have a cusp-locus at the position of the discontinuity for times after a critical value, and the phenomenon is also associated with the appearance of locally sonic flow. It is important to note that the cusp-locus occurs within an expansion in the present situation; it is therefore quite unlike the phenomenon encountered in the formation of 'envelope' shock waves. The flow 'chokes' at the discontinuity in the source distribution after a certain lapse of time and a region of supersonic flow extends downstream from this location and isolates the sources from anything other than strong disturbances that may be generated in the homogeneous (right-hand) parts of the flow. A full discussion is given in Section 6.

2. Equations & Source Terms

The equations of conservation of mass, momentum and energy are written "in conservation form" as

$$\rho_t + (\rho u)_x = G \quad , \tag{2.1}$$

$$(\rho u)_t + (\rho u^2 + p)_x = F \quad , \tag{2.2}$$

$$(\rho E)_t + [\rho u(E + p/\rho)]_x = H \, , \tag{2.3}$$

where

$$E = e + \tfrac{1}{2} u^2 \, , \tag{2.4}$$

and ρ, u, p, e are density, gas velocity, pressure and intrinsic energy. The right-hand sides, G, F, H of (2.1, 2 and 3) represent general sources of mass, momentum and energy.

The square of the local sound speed in the medium is a^2, such that

$$a^2 = \gamma p/\rho \quad , \tag{2.5}$$

where γ is assumed to be a constant. In the circumstances

$$\gamma e = a^2/(\gamma - 1) \, . \tag{2.6}$$

Equations (2.2 and 3) can be rearranged with the aid of (2.4, 5 and 6) to read

$$\rho(u_t + u u_x) + p_x = F - uG \, , \tag{2.7}$$

$$p_t + u p_x - a^2(\rho_t + u \rho_x) = (\gamma - 1)[H - G(E + p/\rho) + u(uG - F)] \tag{2.8}$$

and it is clear that simplifications are provided by a suitable choice of relationships between the various source terms. In particular both (2.7) and (2.8) have zero right-hand sides if

$$F = uG \quad , \tag{2.9}$$

$$H = (E + p/\rho)G \, . \tag{2.10}$$

The latter choice means that (2.8) can be integrated to give

$$p = k(\psi)\rho^{\gamma} \, , \tag{2.11}$$

where $k(\psi)$ is a function of ψ, and a constant value of ψ defines a particle path via the relation

$$\left(\frac{\partial x}{\partial t}\right)_{\psi} = u \, . \tag{2.12}$$

Of course the function $k(\psi)$ is the same as $\exp(s/C_v)$, where s is specific entropy and C_v is the (constant) specific heat at constant volume. It is important to remark that, <u>when the source terms are related as in</u> (2.10 and 11), and provided that the differential-equation system (2.1 - 3) applies, entropy remains constant for any given fluid particle. Restriction to the system (2.1 - 3) means that shock waves, which are not described by these equations, must receive special treatment and <u>will</u> lead to entropy increases in any particle that crosses them in the usual way.

Combination of (2.1) with (2.8) gives

$$p_t + up_x + \rho a^2 u_x = a^2 G \tag{2.13}$$

when (2.9 and 10) apply and, in the same circumstances, the sum of $\pm a$ times (2.7) with (2.13) reveals the characteristics form of the system, namely

$$p_t + (u \pm a)p_x \pm \rho a\left[u_t + (u \pm a)u_x\right] = a^2 G \, . \tag{2.14}$$

Defining the characteristic parameters α, β so that

$$\left(\frac{\partial x}{\partial t}\right)_{\beta} = \frac{x_{\alpha}}{t_{\alpha}} = u + a \, , \tag{2.15a}$$

$$\left(\frac{\partial x}{\partial t}\right)_{\alpha} = \frac{x_{\beta}}{t_{\beta}} = u - a \, , \tag{2.15b}$$

the pair of relations (2.14) can be re-written as

$$(v + u)_\alpha = \bar{c}\, t_\alpha \quad , \tag{2.16a}$$

$$(v - u)_\beta = \bar{c}\, t_\beta \quad , \tag{2.16b}$$

where

$$v = \int dp/\rho a \quad , \tag{2.17}$$

$$\bar{c} = aG/\rho \quad . \tag{2.18}$$

Evidently (2.16a, b) can be integrated, formally at least, but it is helpful to introduce two more postulates before carrying this process through.

3. The Model Problem

First, assume that $k(\nu)$ is constant everywhere within the domain of interest (equivalent to assuming that entropy is similarly constant). As a consequence (2.5, 11 and 17) show that

$$v = \frac{2}{\gamma-1} a \quad . \tag{3.1}$$

Second, assume that the initial state of the gas is such that

$$u = 0 \quad , \quad a = a_0 = \text{constant} \quad ; \quad t = 0$$

over some chosen, sufficiently long, interval in x. Then equations (2.16) integrate to give

$$A + u = \int_0^t \bar{G}\, dt|_\beta \quad , \tag{3.2}$$

$$A - u = \int_0^t \bar{G}\, dt|_\alpha \quad , \tag{3.3}$$

where

$$A \equiv \frac{2}{\gamma-1}(a - a_0) \equiv \frac{2}{\gamma-1} a' \quad , \tag{3.4}$$

and a' is the increment in the local sound speed from its initially constant value a_0. It follows from (3.2 - 4) that (2.15a, b) are equivalent to

$$\left(\frac{dx}{dt}\right)_\beta = a_0 + \tfrac{1}{4}(\gamma+1)\int_0^t \bar{G}\, dt|_\beta + \tfrac{1}{4}(\gamma-3)\int_0^t \bar{G}\, dt|_\alpha \quad , \tag{3.5}$$

$$\left(\frac{dx}{dt}\right)_\alpha = -a_0 - \tfrac{1}{4}(\gamma-3)\int_0^t \bar{G}\, dt|_\beta - \tfrac{1}{4}(\gamma+1)\int_0^t \bar{G}\, dt|_\alpha \quad . \tag{3.6}$$

Evidently the flow field is driven entirely in the present case by the mass sources in $x < 0$.

The model problem in the present case is constructed by assuming that $\bar{G}$ (not G) is a simple piecewise-constant function of x & t.

In particular, the remainder of the present paper will be confined to discussion of the case

$$\begin{aligned} \bar{G} &= \text{constant } (>0), \; x<0; \\ &= 0 \quad , \; x>0. \end{aligned} \tag{3.7}$$

The integrals in (3.2 and 3) are then easily evaluated by calculating the interval of time spent by α & β –characteristics in domains of non-zero $\bar{\sigma}$ up to the chosen time t . The choice of piecewise constant values for $\bar{\sigma}$ is made solely for convenience of calculation in (3.2 and 3), and will be shown to lead to some attractively simple analytical results.

4. Solutions

(a) Region in which presure rises but no flow is induced

Fig. 1 >

Referring to Fig. 1 it can be seen that for any α & β characteristics that lie wholly to the left of the line OC, up to and including time t, (3.2 and 3) give $A \pm u$ both equal to $\bar{a}t$, so that (NB (3.4) for definitions of A & a')

$$u = 0 \quad , \qquad a' = \tfrac{1}{2}(\gamma-1)\bar{G}t \ . \tag{4.1a,b}$$

Since any point in the part of the domain that lies to the left of the line OC is unaware of the spatial nonuniformity in $\bar{G}$ that occurs at $x = 0$ it is not surprising to find that no gas flow is initiated by the source. However, the isentropic efflux from thesource gives rise to a compression when $\bar{G}$ is positive, and it can be confirmed that the sound speed increment in (4.1b) is precisely the same as the one calculated from (2.1) with a zero value for $(\rho u)_x$, coupled with (2.5) and (2.11), with $k(\gamma)$ equal to a constant in the latter.

The line OC is the last α = constant line that lies wholly in $x < 0$; from (3.6 and 7) the equation for OC is simply

$$x = -a_0 t - \tfrac{1}{4}(\gamma-1)\bar{G}t^2 \ . \tag{4.2}$$

(b) Expansion wave travelling into $x < 0$

For any (x,t) point in the domain OCE it can be seen from Fig. 1 that

$$A + u = \bar{a}t \quad , \quad A - u = \bar{G}(t - t_*(\alpha)) \ ; \quad t_*(\alpha) \leq t \ . \tag{4.3a,b}$$

Thus

$$u = \tfrac{1}{2}\bar{G}t_*(\alpha) \ , \tag{4.4a}$$

$$a' = \tfrac{1}{2}(\gamma-1)\left(t - \tfrac{1}{2}t_*(\alpha)\right)\bar{G} \ , \tag{4.4b}$$

where $t_*(\alpha)$ parameterises any particular α = constant line in the OCE domain.

Any α = constant line that lies in OCE , such as the one through D (Fig. 1), has the equation

$$x = -a_0\left[t - t_*(\alpha)\right] - \tfrac{1}{4}(\gamma-1)\bar{C}\left[t^2 - t_*^2(\alpha)\right] + \tfrac{1}{4}(\gamma+1)\bar{C}\,t_*(\alpha)\left[t - t_*(\alpha)\right] . \qquad 4.5$$

It should be observed that u is constant whilst a' increases with time on any such characteristic.

It is interesting to note that

$$\left(\frac{\partial u}{\partial x}\right)_t = \tfrac{1}{2}\bar{C}\left\{a_0 + \tfrac{1}{4}(\gamma+1)\bar{C}t - \bar{C}\,t_*(\alpha)\right\}^{-1} \qquad 4.6$$

in OCE. This velocity gradient is finite, even as t and hence, necessarily, $t_*(\alpha)$ approaches zero in OCE . The magnitude of $(\partial u/\partial x)_t$ diminishes monotonically as t increases.

It is clear that the line OC is the head of an expansion wave that propagates into the uniform domain in $x < 0$, across which there is a jump in the value of u_x from zero (cf (4.1)) to the value $\tfrac{1}{2}\bar{C}\left\{a_0 + \tfrac{1}{4}(\gamma+1)\bar{C}t\right\}^{-1}$.

(c) Compression wave travelling into $x > 0$

Turning now to points within the domain OEG (Fig. 1) it can be seen from (3.2 and 3) that

$$A + u = \bar{C}\,t_*(\beta) \;, \quad A - u = 0 \;; \quad t \geqslant t_*(\beta) .$$

Thus

$$u = \tfrac{1}{2}\bar{C}\,t_*(\beta) = \frac{2}{\gamma-1}\,a' \qquad 4.7$$

and the equation of a constant-β line in OEG , such as the one through the point F, is

$$x = \left\{a_0 + \tfrac{1}{4}(\gamma+1)\bar{C}\,t_*(\beta)\right\}\left[t - t_*(\beta)\right] . \qquad 4.8$$

The velocity gradient is given by

$$\left(\frac{\partial u}{\partial x}\right)_t = -\tfrac{1}{2}\bar{C}\left\{a_0 + \tfrac{1}{2}(\gamma+1)\bar{C}\,t_*(\beta) - \tfrac{1}{4}(\gamma+1)\bar{C}t\right\}^{-1} \qquad 4.9$$

in these circumstances.

The flow in OEG, at least for early times, is undergoing isentropic compression through a simple wave, as testified by the straight-line character of the constant-β line in (4.8), for example. The unperturbed field in $x > 0$ into which the simple wave propagates is a field with constant sound speed a_0

and zero flow velocity. The wave-head OG is given by $x = a_0 t$ (put $t_*(\beta) = 0$ in 4.8)), and the simple isentropic compression wave that follows it will only continue as such until u_x becomes unbounded. This occurs on the simple-wave head at the time t_{sh}; (4.9) shows that

$$t_{sh} = 4a_0/(\gamma+1)\bar{G} \ . \qquad 4.10$$

More will be said about the shock wave, that must now lead the flow into the right-hand domain $x > 0$, in due course.

Meanwhile it is important to observe a key feature of the flow field that occurs, and remains, at least for some time, at the location $x = 0$ of the discontinuity in the source distribution $\bar{G}$. On any line of constant-α or constant-β, such as (4.5) or (4.8) in present circumstances, x approaches zero as t approaches either $t_*(\alpha)$ or $t_*(\beta)$. Moreover, if $t_*(\alpha)$ is equal to $t_*(\beta)$, $x = 0$ can be approached from either the left (on α = constant) or the right (on β = constant) at the same instant of time by letting $t \to t_*(\alpha) = t_*(\beta)$.

First of all it is important to note from (4.4) and (4.7) that u & a' are continuous at $x = 0$. Second, it can be seen from (4.6) and (4.9) that

$$\left(\frac{\partial u}{\partial x}\right)_t \to \tfrac{1}{2}\bar{G}\left\{a_0 - \tfrac{1}{4}(3-\gamma)\bar{G}t\right\}^{-1}, \quad x \to 0- \ ; \qquad 4.11$$

$$\left(\frac{\partial u}{\partial x}\right)_t \to -\tfrac{1}{2}\bar{G}\left\{a_0 + \tfrac{1}{4}(\gamma+1)\bar{G}t\right\}^{-1}, \quad x \to 0+ \ . \qquad 4.12$$

Thus flow-velocity gradient suffers a discontinuous change across $x = 0$ from positive and increasing magnitude as t increases in $x < 0$ to negative and decreasing magnitude in like circumstances in $x > 0$.

It can be seen from (4.7) that $(\partial a'/\partial x)_t$ is always equal to $\frac{1}{2}(\gamma-1)$ times $(\partial u/\partial x)_t$ in the domain OEG, whence the value of $(\partial a'/\partial x)_t$ as $x \to 0+$ is evident from (4.12). However it is necessary to calculate $(\partial a'/\partial x)_t$ in OCE from (4.4 and 5). The result is readily seen to be

$$\left(\frac{\partial a'}{\partial x}\right)_t = -\tfrac{1}{4}(\gamma-1)\bar{G}\left\{a_0 + \tfrac{1}{4}(\gamma+1)\bar{G}t - \bar{G}t_*(\alpha)\right\}^{-1} \ . \qquad 4.13$$

It therefore follows that as $x \to 0-$ in OCE (which is achieved by letting $t \to t_*(x)$ in (4.13)),

$$\left(\frac{\partial a'}{\partial x}\right)_t \to -\tfrac{1}{4}(\gamma-1)\bar{G}\left\{a_0 - \tfrac{1}{4}(3-\gamma)\bar{G}t\right\}^{-1}. \qquad 4.14$$

Thus a' and hence, in view of the isentropic character of the flow at this stage, pressure and density too, will suffer a discontinuity in slope, but not value, as x crosses $x = 0$.

(d) The critical time t_c and the appearance of sonic flow

It is observed from (4.11) and (4.14) that both $|u_x|$ and $|a'_x|$ at $x = 0-$ grow without bound as the time t increases towards a value t_c given by $4a_0/(3-\gamma)\bar{G}$. This remark relating to conditions as $x \to 0-$ is made on the supposition that $\gamma < 3$, as indeed must be the case for gases. It is therefore reiterated that $|u_x|$ & $|a'_x| \to \infty$ simultaneously as $x \to 0$ and $t \to t_c$, both from below, where

$$t_c = 4a_0/(3-\gamma)\bar{G}. \qquad 4.15$$

As with the shock-wave that forms at time t_{sh} it is necessary to say more (below) about what happens at and after t reaches t_c. Meanwhile, note that

$$t_c > t_{sh} \qquad 4.16$$

is always true since γ always exceeds unity.

It is important for the interpretation of what happens to the flow field at and after time t_c to remark that when $t = t_c$, u at $x = 0$ is the same as a at that location, since u is equal to $\frac{1}{2}\bar{G}t$ and a' is equal to $\frac{1}{4}(\gamma-1)\bar{G}t$ at $x = 0$, $0 \le t \le t_c$, as can be seen from (4.4) or (4.7). Thus locally sonic flow is first achieved at $x = 0$, $t = t_c$.

(e) Summary of the main results so far

The principal results in this Section can be summarised in the form of the elementary relationships that exist between u, a, x & t that are implicit in (4.4 and 5) and (4.7 and 8). Thus, in OCE

$$x = -\left\{a_0 - u + \tfrac{1}{4}(\gamma-1)\bar{G}t\right\}\left(t - \frac{2u}{\bar{G}}\right), \qquad 4.17$$

$$a = a_0 + \tfrac{1}{2}(\gamma-1)(\bar{C}t - u) , \qquad 4.18$$

whilst in

$$x = \left\{ a_0 + \tfrac{1}{2}(\gamma+1)u \right\}\left(t - \frac{2u}{\bar{C}}\right) , \qquad 4.19$$

$$a = a_0 + \tfrac{1}{2}(\gamma-1)u . \qquad 4.20$$

(f) Illustrative results

Fig.2&3 >

Figs. 2 and 3 illustrate the gas velocity and sound-speed distributions at a time equal to 0.8 of the value t_c (eq. (4.15)) for γ equal to $7/5$. The time t_{sh} at which a shock-wave forms (at the right-hand end of the flow field) is equal to $\frac{2}{3}t_c$ under these circumstances. The multi-valuedness that is apparent in both velocity u and sound speed a is therefore to be expected; it is discussed in sufficient detail in Section 5 below, not primarily in connection with the apperance of an "envelope" shock itself, which is not a new phenomenon, but more for the influence that this will have on the domain of isentropic flow.

The imminent appearance of multi-valuedness in both u and a at $x=0$ at and after time t_c is apparent on both Figs. 2 and 3. This heralds the approach of a new phenomenon, that is to be fully described and analysed in Section 6. That this new phenomenon is associated, not with a compression as in $x>0$, but with an expansion process, can be appreciated from the different combinations of u and a variations in $x<0$ and in $x>0$.

5. The Shock Wave

The shock that forms at time t_{sh} (see (4.10)) on $x = a_o t$ means that the condition of isentropic behaviour will be violated in the flow field from that moment on. However the region of strictly non-isentropic flow must be bounded, on the right by the shock itself, of course, and on the left by the α-characteristic that passes through the point $t = t_{sh}$, $x = a_o t_{sh}$. Fig. 4 is a sketch of the situation that incorporates some of the facts already elicited in Section 4 as well as some that must be validated here. This is particularly true of the shape and disposition of the two α-lines CB, for which α has the value α_1, and SA for which α is given by α_2.

Fig. 4

Since it is equal to $u - a$, the derivative $(\partial x/\partial t)_\alpha$ is zero when u is equal to a; this locally sonic state is first achieved when t is t_c on the line $x = 0$ (cf remarks that follow (4.16)). Thus characteristic α_1 is tangent to the t-axis at point C; its shape (as sketched in Fig. 4) between C and point B, where it intersects the isentropic-compression wave-head, is consistent with the known behaviour in domain OEG (see Section 4(c)).

The constant-β line, $\beta = \beta_s$, that passes through point C is characterised by a constant value of u in $x \geq 0$ given by $\frac{1}{2}\bar{G}t_c$ (see (4.7)). In view of (4.15) this value is $2a_o/(3-\gamma)$, and it is readily seen from (4.7) that $a_o + a'$, or a, has precisely this same value. Thus the β_s-line is a characteristic line that is also a sonic line, as indicated on Fig. 4. If the α_2-line emanating from the shock-formation point S lies to the right of α_1, as in the sketch, it will intersect β_s at A with zero value of $\partial x/\partial t$, and the region of non-isentropic flow produced by the shock will remain in $x > 0$. This supposes, as does Fig. 4, that $u > a$ for t-values above the line CA. Both this supposition and the one about the relative dispositions of points B and S can be substantiated, as will now be seen.

(a) The shape of the α-characteristics in $x > 0$

It is clearly necessary to calculate the shape of α-lines in the OEG domain (Fig. 1) in order to resolve the issues raised above. From (2.15b) and (4.7),

$$\left(\frac{\partial x}{\partial t}\right)_\alpha = -a_o + \tfrac{1}{2}(3-\gamma)u \,. \qquad 5.1$$

The relationship between u, x & t is found from (4.19) to be

$$(\gamma+1)u^2 + \left(2a_0 - \tfrac{1}{2}(\gamma+1)\bar{G}t\right)u + (x - a_0 t)\bar{G} = 0 \quad . \qquad 5.2$$

Solving this equation for u, and taking the positive sign for the square root, leads to the following differential equation for the variation of x with t on a constant-α line in OEG ;

$$\left(\frac{\partial x}{\partial t}\right)_\alpha = -a_0 + \tfrac{1}{8}(3-\gamma)\bar{G}\left\{t - t_{sh} + \sqrt{(t+t_{sh})^2 - 4x t_{sh} a_0^{-1}}\right\} . \qquad 5.3$$

The manipulations required to solve (5.3) are described in Appendix A. Although general conclusions, for any value of γ, are not accessible from the solution it is easy enough to demonstrate by direct numerical calculation that the lines α_1 & α_2 for $\gamma = 7/5$ are in the positions depicted in the sketch in Fig. 4 (see Fig. A.1 for the numerical results).

Thus the assertions implicit in Fig. 4 regarding the domain of non-isentropic flow are substantiated when $\gamma = 7/5$.

(b) Estimate of shock path for times near to t_{sh}

Validation of the idea that $u > a$ in the region above the line in Fig. 4 will be undertaken in the next Section. The present Section will be closed with some observations about the character of the shock that forms at time t_{sh} on $x = a_0 t$. Initially the shock will be very weak and the changes of entropy from one particle-path that crosses the shock to another will be small enough to be neglected, at least in a first approximation. The isentropic simple compression-wave will provide an adequate description of conditions behind the shock in these circumstances, and the weak-shock-fitting theory of Whitham (1974, §2.8) can be used to show that the shock follows a path

$$x = x_{sh}(t) \equiv a_0\left\{t + \tfrac{3}{8}t_{sh}\left(\frac{t}{t_{sh}} - 1\right)^2\right\} , \qquad 5.4$$

at least in the early part of its history. The real finite-amplitude wave will run ahead of the path (5.4) as t more and more exceeds t_{sh} .

6. Cusp Locus for α-characteristics*

Continuation of the solutions derived in Section 4 into times in excess of t_c (see (4.15)) must be done with some care, at least in the neighbourhood of $x=0$. Integration of $\bar{G}$ along a line of constant β, as required by (3.2), is straight-forward and $A+u$ is equal to $\bar{G}\,t_*(\beta)$ for any points that lie to the right of $x=0$ when $t_*(\beta)$ exceeds t_c. This situation is illustrated in Fig. 4, which supposes that $u \geq a$ in the region DCAFE. Any constant-α line, such as one that lies between α_1 & α_2, for example, must have x_t equal to zero where it crosses the β_s line, as explained in Section 5. Regardless of the direction that it takes after crossing CA on β_s, this same line must continue for some time in $x>0$ and, accordingly, (3.3) makes A equal to u on the α-line immediately above CA. Thus

$$A = u = \tfrac{1}{2}\bar{G}\,t_*(\beta)$$

for $t_*(\beta) > t_c$, whence $u > a$ as a sole consequence of the excess of $t_*(\beta)$ over t_c. It follows that x_t on a line of constant α above CA must be positive and the α-lines in this domain must be as sketched in Fig. 4, including α_1.

Now consider those α-lines that cross from $x>0$ into the domain $x<0$. It is clear from the analysis to date that this can certainly happen for $t_*(\alpha)$ values (see Fig. 1) less than t_c. Solutions for u & a' under these conditions are found in equations (4.4), which together show that

$$a-u = a_0 + \tfrac{1}{2}(\gamma-1)\bar{G}t - \tfrac{1}{4}(\gamma+1)\bar{G}\,t_*(\alpha)\,. \qquad 6.1$$

It is evident from (4.4) that a is least when t is least, and equal to $t_*(\alpha)$ in the present case; (6.1) then makes

$$a-u = a_0 - \tfrac{1}{4}(3-\gamma)t_*(\alpha) \geq 0\,, \quad t = t_*(\alpha) \leq t_c\,,$$

and u is therefore less than a on any α-line that crosses into $x \leq 0$ for $t_*(\alpha) < t_c$. Evidently $u=a$ at $x=0$ when $t_*(\alpha)=t_c$, with $u<a$ everywhere else along this α-line in $x<0$. Accordingly, the slope x_t of all α-lines with $t_*(\alpha) < t_c$ is negative in $x \leq 0$; when $t_*(\alpha)=t_c$, $x_t \leq 0$, with equality occuring only at $x=0$.

The situation in the neighbourhood of the critical point $x=0, t=t_c$, as revealed so far, is sketched in Fig. 5. The characteristic α_1 has a cusp at the point C and continues in $x>0$ along α_1+ and in $x<0$ along α_1-. It appears that no α-line emanating from the initial line can penetrate into

---

* This particular cusp locus should not be confused with a limit line (von Mises, 1958, Art. 19).

the region between α_1+ & α_1-. However, this remark ignores the character of the source distribution given in (4.1), for which $\bar{G}$ is undefined at $x = 0$.

It is useful to think of $\bar{G}$ as a continuous function that decays rapidly, from a constant non-zero value in $x<0$ to zero in $x>0$ in the near neighbourhood of $x=0$. Then α-characteristics in a near neighbourhood of α_1 will pass through this region of continuous change in $\bar{G}$, centred around $x=0$, as a continuous distribution of curves covering the whole space between α_1- and α_1+. This situation must persist as the spatial interval within which $\bar{G}$ changes from its constant value to zero shrinks towards zero around $x = 0$.

The α-characteristics in-between $\alpha_1 \pm$ must all enter this region at the cusp C (Fig. 5) in the limiting case for which the region within which $\bar{G}$ varies shrinks to zero-size around $x = 0$. These characteristics must eventually emerge into either $x<0$ or $x>0$ having, in general, spent some time within the bundle of characteristic lines that follow the t-axis above C. At this stage it is not possible to assess the contribution to $\int \bar{G}\,\delta t|_{\alpha}$ that will arise from this time spent within the domain of changing $\bar{G}$. However, it must be remarked that <u>if</u> this time (and hence contribution to the integral) turns out to be zero, then all α-lines in $\alpha_1 \pm$ must emanate from C. There are good reasons for supposing this <u>not</u> to be the case, based on the conclusion from (4.4), with t_c in place of $t_*(\alpha)$, that u between α_1- & $x=0$ will then remain constant at the value $\frac{1}{2}\bar{G}t_c$; such a conclusion is, at the least, physically implausible. The simple analysis that follows will be seen to resolve all such matters in a satisfactory way.

Consider the line $\alpha-$ that emerges into $x<0$ at time $t_*(\alpha)$ at point $\mathcal{L}$ (Fig. 5). For any point on $\alpha-$ above $\mathcal{L}$ (3.2 and 3) give (NB $t \geq t_*(\alpha)$.)

$$A + u = \bar{G}t \quad , \tag{6.2a}$$

$$A - u = \bar{G}[t - t_*(\alpha)] + F(\alpha) \quad , \tag{6.2b}$$

where $F_-(\alpha)$ is the value, unknown at this stage, of $\int \bar{C}\,\partial t|_\alpha$ between t_c & $t_*(\alpha)$. A similar evaluation for any point on $\alpha+$ above $\mathcal{B}$ gives

$$A + u = \bar{C}\, t_*(\beta) \ , \qquad 6.3a$$

$$A - u = F_+(\alpha) \ , \qquad 6.3b$$

where $F_+(\alpha)$ is the value of $\int \bar{C}\,\partial t|_\alpha$ for the $\alpha+$ characteristic, and $t \geq t_*(\alpha)$.

If both $\alpha+$ & $\alpha-$ are to spend the time between points C and $\mathcal{B}$ on the t-axis, $(\partial x/\partial t)_\alpha$ must be zero there in both cases, and (2.15b) shows that u must be equal to a in this segment of the axis. In particular, choose t equal to $t_*(\alpha)$ on $\alpha-$ & on $\alpha+$ (so that $t_*(\beta)$ is also equal to t). Then (6.2 and 3) show that

$$F_-(\alpha) = \left(\frac{3-\gamma}{\gamma+1}\right)\bar{C}\, t_*(\alpha) - \frac{4}{\gamma+1}\, a_0 = F_+(\alpha) \equiv F(\alpha) \ . \qquad 6.4$$

Using the definition of t_c from (4.15), (6.4) can be rewritten as

$$F(\alpha) = \frac{4}{\gamma+1}\, a_0 \left(\frac{t_*(\alpha)}{t_c} - 1 \right) \ . \qquad 6.5$$

An important conclusion from (6.4) is that u and A (and hence p, ρ, etc) must be continuous at $x = 0$ in the present domain above point C. Characteristics such as $\alpha\pm$ emerge from cusps at $\mathcal{B}$, just as the limiting $\alpha_1\pm$ characteristics do from C.

The time-axis above C is therefore a locus of cusps for the α-characteristics. In addition, of course, this portion of the axis is a sonic line.

It is now necessary to evaluate the complete character of the field in between the characteristics $\alpha_1\pm$, starting with the situation in $x < 0$.

(a) <u>The field in $x < 0$</u>

It follows at once from (6.2, 4 and 5) that

$$u = \left(\frac{2}{3-\gamma}\right) a_0 \frac{t_*(\alpha)}{t_c} - \left(\frac{2}{\gamma+1}\right) a_0 \left(\frac{t_*(\alpha)}{t_c} - 1 \right) \ , \qquad 6.6a$$

$$a = a_0 + \left(\frac{\gamma-1}{3-\gamma}\right) a_0 \left(2\,\frac{t}{t_c} - \frac{t_*(\alpha)}{t_c} \right) + \left(\frac{\gamma-1}{\gamma+1}\right) a_0 \left(\frac{t_*(\alpha)}{t_c} - 1 \right) \ , \qquad 6.6b$$

where $t \geq t_*(\alpha) \geq t_c$. Thus u is constant on any given α-line, and increases with increasing $t_*(\alpha)$ (cf Fig. 5). The flow defined by (6.6) is subsonic.

The shape of the α-lines in the present domain is found from (2.15b) and (6.6);

$$x t_c = -\left(\frac{\gamma-1}{3-\gamma}\right)\left[t - t_*(\alpha)\right]^2 a_0 \ . \qquad 6.7$$

Since u in (6.6a) depends only upon $t_*(\alpha)$, (6.7) can be rewritten to provide an implicit relationship for u as a function of x,t in the present domain.

The general expression for $(\partial u/\partial x)$ at fixed t is particularly simple in the present case, since it is found from (6.6 and 7) that

$$\left(\frac{\partial u}{\partial x}\right)_t = 2/(\gamma+1)\left[t - t_*(\alpha)\right] \ . \qquad 6.8$$

Fig. 5 makes it clear that as $t_*(\alpha)$ approaches t_c from above, points on α-approach points on α_1- from within the $\alpha_1 \pm$ domain or, in other words, from the right. One can approach this same point on α_1- from the left by letting $t_*(\alpha)$ in (4.6) approach t_c from below; eliminating $\bar{C}_3$ in the resulting expression by using (4.15) it can be demonstrated that $(\partial u/\partial x)_t$ is the same, and equal to

$$2/(\gamma+1)(t - t_c) \ ,$$

whichever way one approaches α_1-.

Note that $(\partial u/\partial x)_t$ becomes unbounded as one approaches $x = 0$ from $x < 0$, since Fig. 5 makes it plain that $t \to t_*(\alpha)$ in such circumstances; the result follows from (6.8).

Fig. 6 >

The various features of the flow that have been described in this section are illustrated for a specific case $t > t_c$ in Fig. 6.

(b) The field in $x > 0$

The results in (6.3, 4 and 5) show that in $x > 0$

$$u = \left(\frac{2}{3-\gamma}\right) a_0 \frac{t_*(\beta)}{t_c} - \left(\frac{2}{\gamma+1}\right) a_0 \left(\frac{t_*(\alpha)}{t_c} - 1\right) \ , \qquad 6.9a$$

$$a = a_0 + \left(\frac{\gamma-1}{3-\gamma}\right) a_0 \frac{t_*(\beta)}{t_c} + \left(\frac{\gamma-1}{\gamma+1}\right) a_0 \left(\frac{t_*(\alpha)}{t_c} - 1\right) \ . \qquad 6.9b$$

It is clear that in the present domain, between $x=0$ and the α_1+ line, the situation is more complicated than elsewhere in the present problem since u and a depend upon both α and β. This means that (2.15a and b) give

$$x_\alpha = \left\{ \frac{4}{\gamma+1} - \left(\frac{3-\gamma}{\gamma+1}\right)\frac{t_*(\alpha)}{t_c} + \left(\frac{\gamma+1}{3-\gamma}\right)\frac{t_*(\beta)}{t_c} \right\} a_0 t_\alpha \ , \qquad 6.10a$$

$$x_\beta = \left\{ \frac{t_*(\beta)}{t_c} - \frac{t_*(\alpha)}{t_c} \right\} a_0 t_\beta \ , \qquad 6.10b$$

and it is not a trivial matter to simultaneously integrate this pair of equations. The method used to find u and a (or v) as functions of x and t is described in Appendix B. The results, (B12 and 13), give the answer in implicit form. Examples of the velocity and sound-speed distributions in the space between $x=0$ & $\alpha=\alpha_1+$, derived by the methods described in Appendix B, are given in Fig. 7 for the same conditions as those used to construct Fig. 6.

Fig.7>

(c) General properties of the solution near α_1+

It is important to examine behaviour in the neighbourhood of α_1+ in a more general way than can be done through the medium of essentially illustrative numerical results.

To start with, u and a' must still obey (4.7) in the domain $\beta>\beta_s, \alpha>\alpha_1+$. Since the actual path taken by a β-line in the space between $x=0$ & $\alpha=\alpha_1+$ is not readily calculable, being concealed in the rather awkward implicit results given in Appendix B, the β-lines in $\beta>\beta_s$, $\alpha>\alpha_1+$, do not obey (4.8), although (4.7) guarantees that they will be straight lines. Recalling (4.15), it is clear that u & a are continuous across α_1+, as can be seen by comparing (4.7) with (6.9), with $t_*(\alpha)$ equal to t_c in the latter. Gradients, such as $(\partial u/\partial x)_t$ for example, are <u>not</u> continuous at α_1+, as shown in Fig. 7 and as we now proceed to demonstrate.

It can be shown that

$$2a\,(u_x)_t = (u_t)_\beta - (u_t)_\alpha \ .$$

Writing $[f]$ to indicate the jump in f across an α-characteristic, it follows from the continuity of u & a that

$$2a\,[(u_x)_t] = [(u_t)_\beta]$$

on α_1+. But (4.7) shows that $(u_t)_\beta$ is zero in $\alpha > \alpha_1+$, whilst (6.9a) shows that, in $\alpha < \alpha_1+$,

$$(u_t)_\beta = -\{2a_0/(\gamma+1)\}\ \dot{t}_*(\alpha)/t_c\ \},$$

where $\dot{t}_*(\alpha)$ is the time-rate-of-change of $t_*(\alpha)$ on a line of fixed β. It is evident from Fig. 3 that $\dot{t}_*(\alpha) < 0$, whence $(u_t)_\beta > 0$ in $\alpha < \alpha_1+$, and

$$[(u_x)_t] < 0. \qquad 6.11$$

The result in (6.11) is general, and indicates that the general form of the profiles of u and a versus x at a fixed t, exemplified in Fig. 7, will persist for $t > t_c$ on α_1+.

(d) The β-characteristics in $\beta > \beta_s$, $\alpha > \alpha_1+$

It should be noted that the shape of the line α_1 is (properly) found as described in Appendix A for β-values less than β_s (Fig. 5). When $\beta > \beta_s$, and the α-characteristics are cusped on $x = 0$, their shape in x, t space will be deducible from the work of Appendix B. In view of the continuity of u and a at α_1+ it must follow that $(\partial x/\partial t)_{\alpha_1+}$ is as shown in (5.1), whether one approaches α_1+ from the left or right. Thus the line α_1+ can be continued into $\beta > \beta_s$ by the integration described in Appendix A.

The β-lines in $\beta > \beta_s$, $\alpha > \alpha_1+$ must now be found from

$$x - x_+(\beta) = \left\{1 + \left(\frac{\gamma+1}{3-\gamma}\right)\frac{t_*(\beta)}{t_c}\right\} a_0\left(t - t_+(\beta)\right), \qquad 6.12$$

where x_+, t_+ is a point on α_1+ (Fig. 5) that changes with change in β.

Fig. 7 shows the behaviour of u as a function of x at a fixed time t, as calculated from (6.12) and (4.7). The result is given by the full line to the right of α_1+ and, for comparison, a calculation made with (4.8) is indicated by the dashed line in Fig. 7. The difference between the two results is certainly small and the error committed by using (4.8) in place of the correct result in (6.12) is not large at the chosen time. Clearly the discrepancy will increase as t increases, and even the small difference on Fig. 7 is interesting insofar as it demonstrates that the influence of the advent of sonic conditions at $x = 0$ for $t \geq t_c$ extends into the domain bounded on the right by β_s (Fig. 5).

Finally, note the position of characteristic α_2 on Fig. 7; to the left of α_2 the flow remains isentropic, as explained in Section 5. To the right of α_2 the shock, whose strength is rising steadily with increasing time, makes the real flow non-isentropic; the analytical predictions must begin to fail in these regions.

7. Conclusions

By choosing a particular form for the source terms that appear in the conservation equations for continuous compressible one-dimensional unsteady motion an exact solution for the whole source-driven flow field has been derived, up to the time of shock formation at the right-going wavehead. The consequent domain of non-isentropic flow has been determined.

Exact solutions have been continued into times up to and beyond the appearance of sonic flow, which is associated with some novel characteristic behaviour at part of the sonic locus, where the characteristics are cusped. The flow out of the source regions 'chokes', after a lapse of time that depends on source strength (see (4.15)), at the plane $x = 0$ which marks the division in the field between 'sources' and 'no sources'. Provided that source-output continues, a widening patch of supersonic flow extends downstream of $x = 0$, eventually extending up to the shock wave. This has the effect of insulating the source region from anything other than strong disturbances, that may be created in $x = 0$ (e.g. by ending the tube, in which the flows described here are presumed to be confined, and discharging into an ambient atmosphere). The fact that the sources (or propellants) can continue to discharge gas unhampered by any but strong external influences can have important practical consequences.

The exact solutions contain a number of salient features, which means that they also provide a useful problem on which to test numerical algorithms.

References

Krier, H. & Summerfield, M. (1979). "Interior Ballistics of Guns", Prog. in Astro. & Aeronautics, Vol. 66. AIAA, New York.

von Mises, R. (1958) "The mathematical theory of compressible fluid flow", completed by Hilda Geiringer and G.S.S. Ludford. Academic Press, New York.

Roe, P.L. (1986) "Characteristic-Based Schemes for the Euler Equations", Ann. Rev. Fluid Mech., 18, 337-365.

Whitham, G.B. (1974) "Linear and nonlinear waves". John Wiley, New York.

Figure Captions

Fig. 1 The characteristic families α = constant and β = constant on the x,t diagram. The figure also defines the parameters $t_*(\alpha)$ and $t_*(\beta)$.

Fig. 2 Gas velocity u as a fraction of the initial unperturbed sound speed a_0 versus $x/a_0 t_c$, where t_c is defined in (4.15), at time $t = 0{\cdot}8\, t_c$ and $\gamma = 1{\cdot}4$. The picture is broadly typical of all times up to, but not beyond, $t = t_c$. Multivaluedness only exists at the right-hand end of the wave system for $t > \frac{2}{3} t_c$. The changes that appear at $x=0$ for $t = t_c$, and spread into $x \gtrless 0$ for $t > t_c$ are explained in Section 6 and illustrated in Figs. 6 and 7.

Fig. 3 As for Fig. 2, with a/a_0 in place of u/a_0 where a is the local sound speed.

Fig. 4 Disposition of some critical flow-field features associated with the appearance of the shock wave.

Fig. 5 Characteristic lines on the x,t plane in the neighbourhood of the cusp locus.

Fig. 6 Gas velocity versus distance in $x < 0$ for $t > t_c$. The full line shows the exact solution derived from (6.6a) and (6.7) for time $t = 2{\cdot}1798\, t_c$. The dashed line is calculated from (4.17) and is exact to the left of α_1- at this same time.

Fig. 7 Gas velocity and local sound speed in $x > 0$ for $t > t_c$. The exact solutions are indicated by the full lines for time $t = 2{\cdot}1798\, t_c$; between $x = 0$ and α_1+ the solutions are found in the manner described in §6(b) and Appendix B; for positions to the right of α_1+ they are found from (6.9) and (6.12). The dashed line is calculated from (4.8).

Between α_2 and the shock the flow is not isentropic; the full-line curves no longer give the exact solution.

Note that the whole flow, between the "throat" at $x = 0$ and the shock is supersonic for the particular case illustrated.

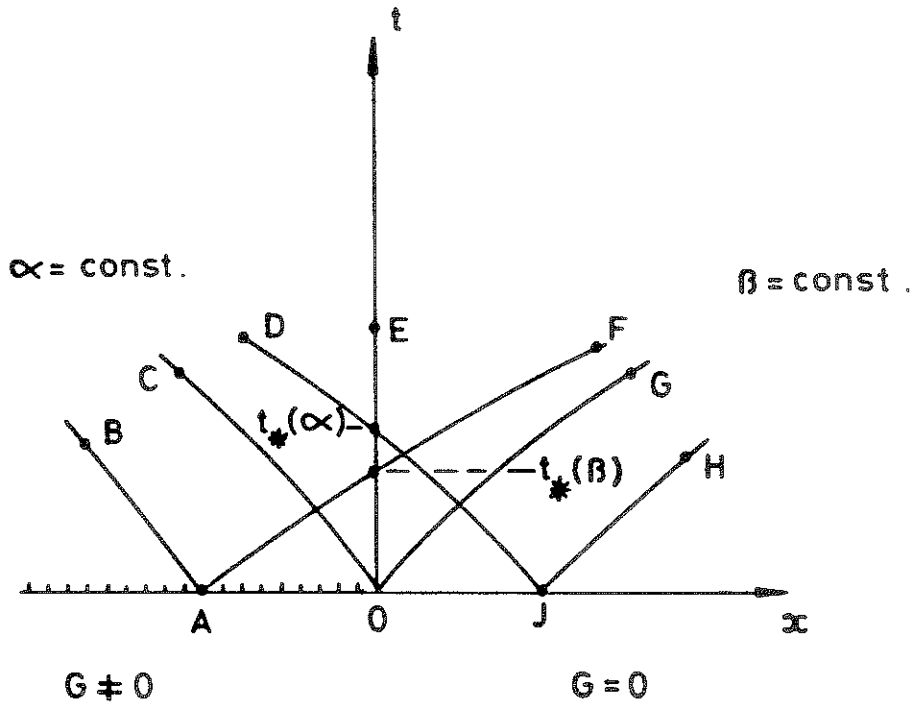

Fig. 1.

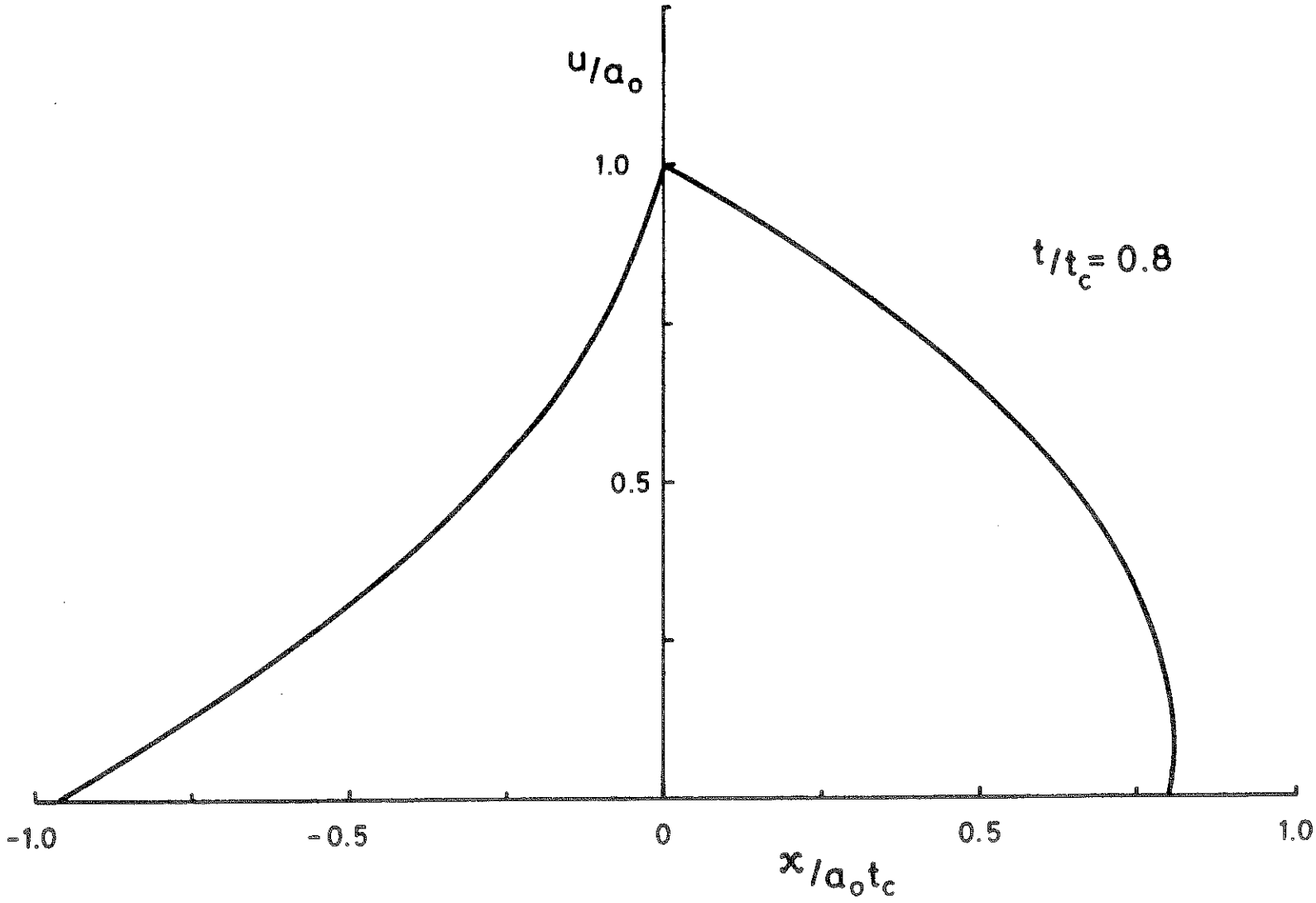

Fig. 2.

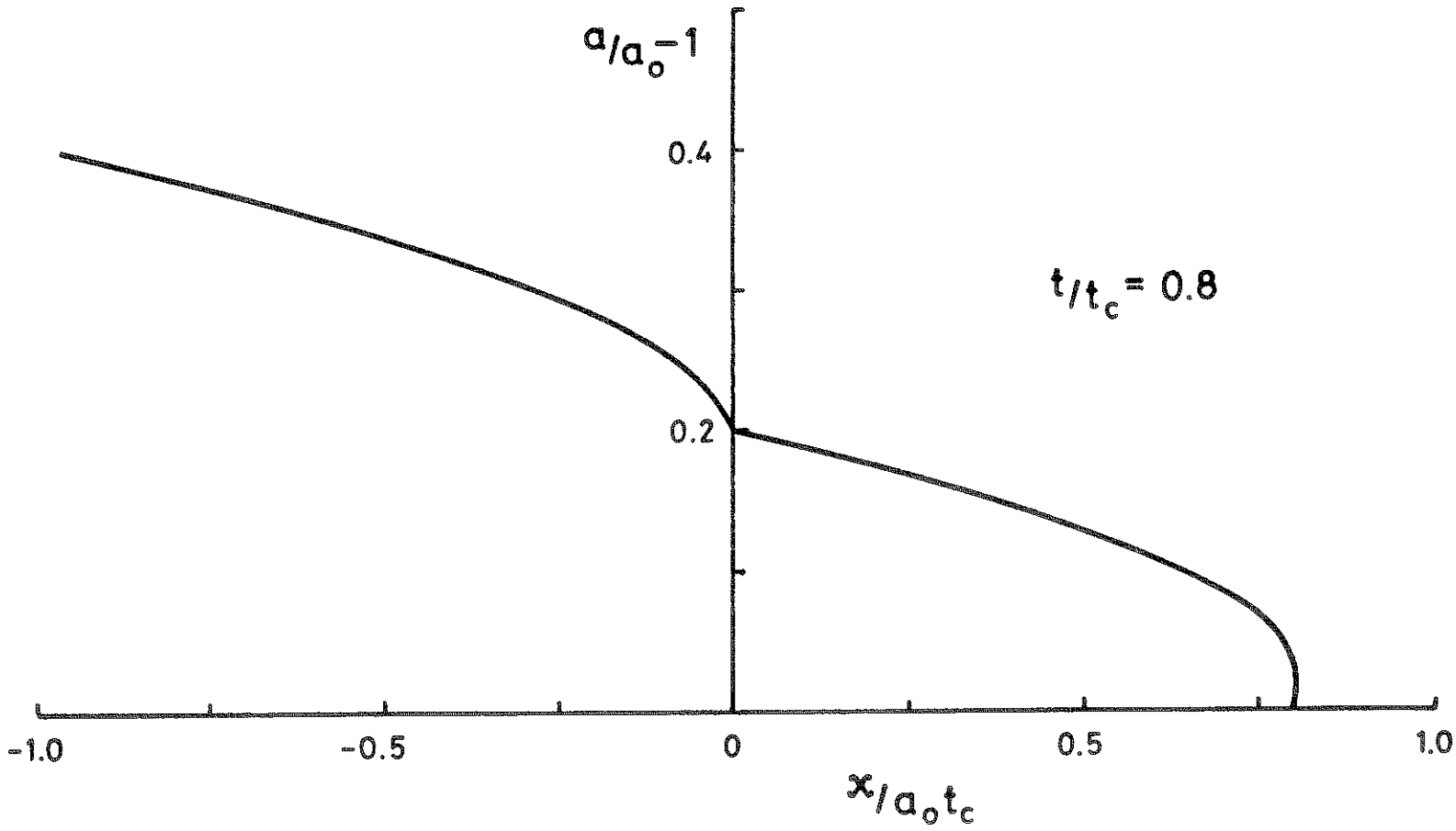

Fig. 3.

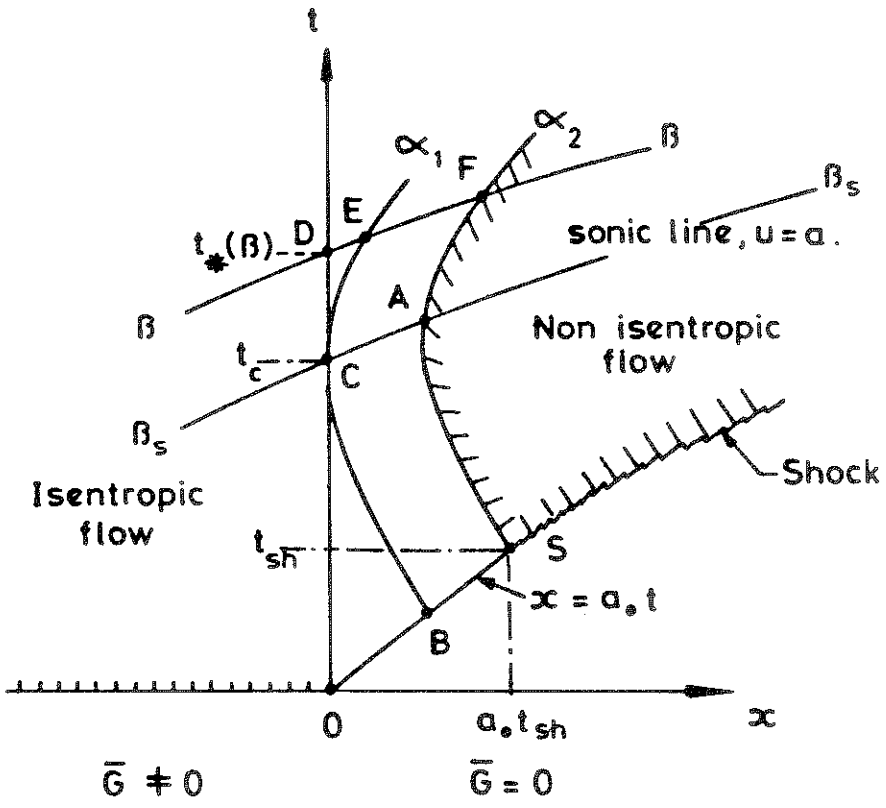
t
α_1
F
α_2
ß
$ß_s$
E
D
$t_*(ß)$
sonic line, u = a.
A
ß
Non isentropic
flow
t_c
C
$ß_s$
Shock
Isentropic
flow
t_{sh}
S
$x = a_* t$
B
0
$a_* t_{sh}$
x
$\bar{G} \neq 0$
$\bar{G} = 0$

Fig. 4.

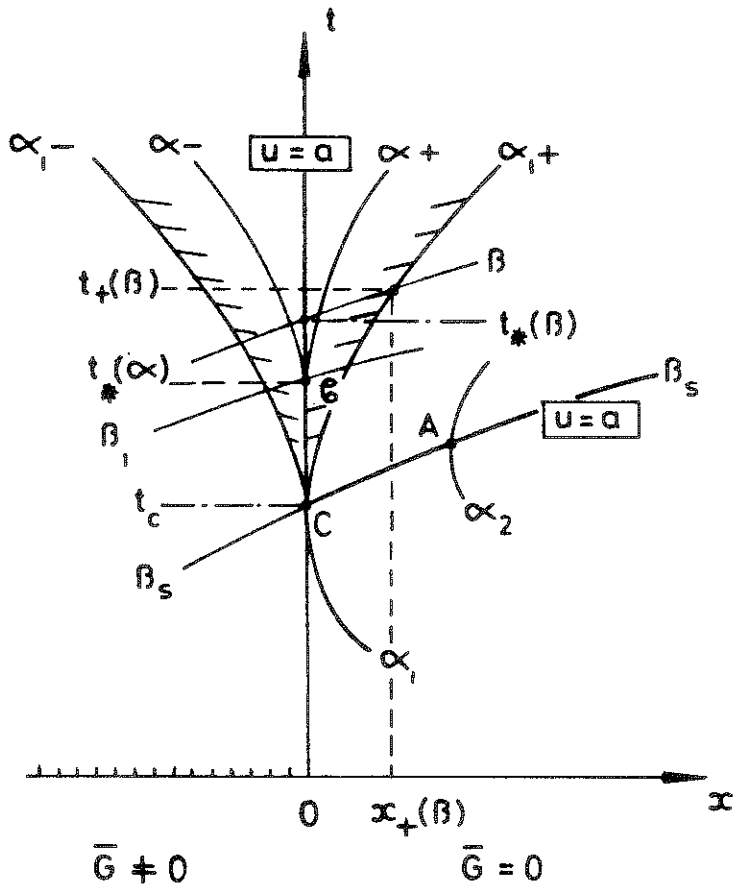

Fig.5.

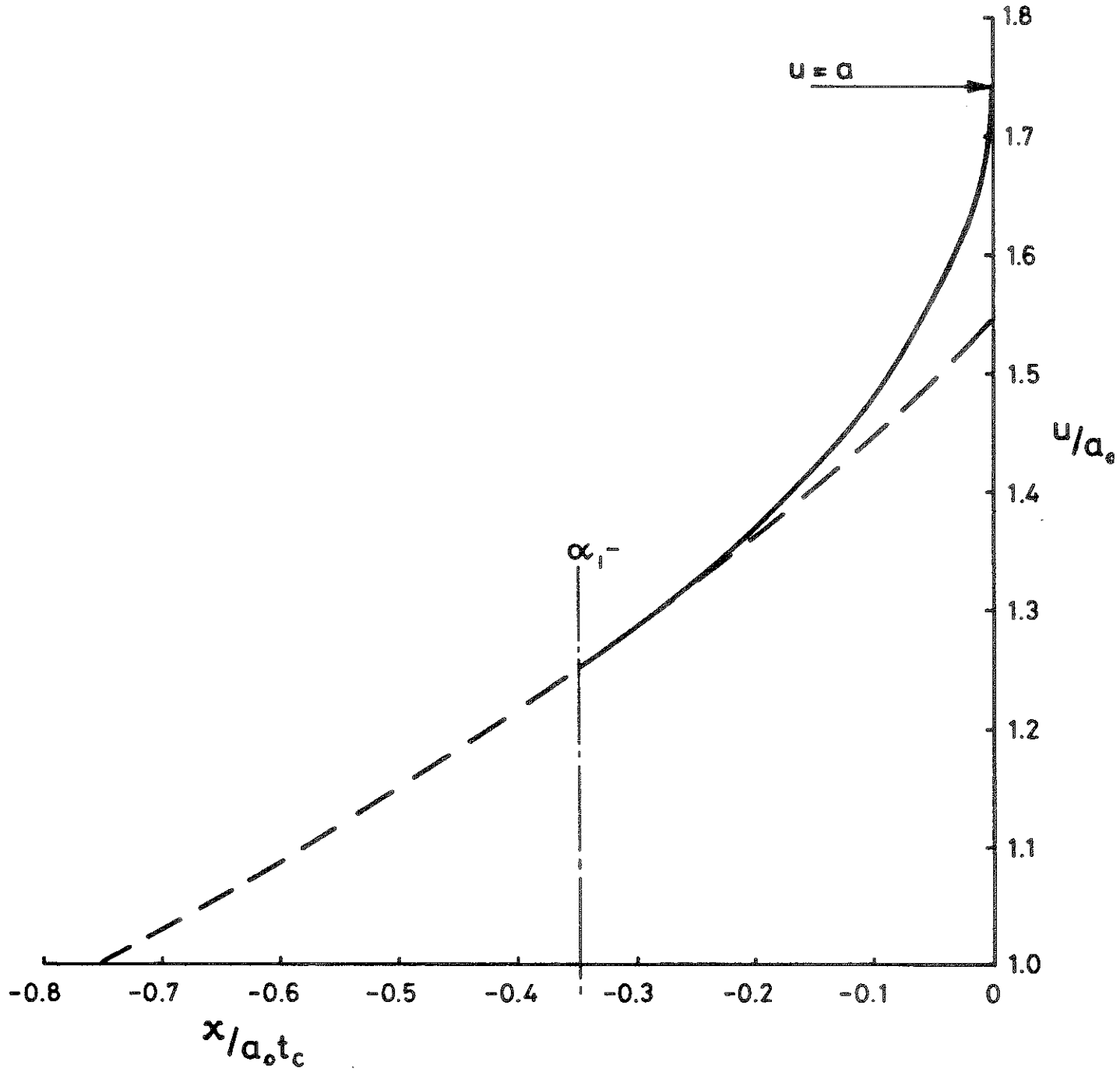

Fig. 6.

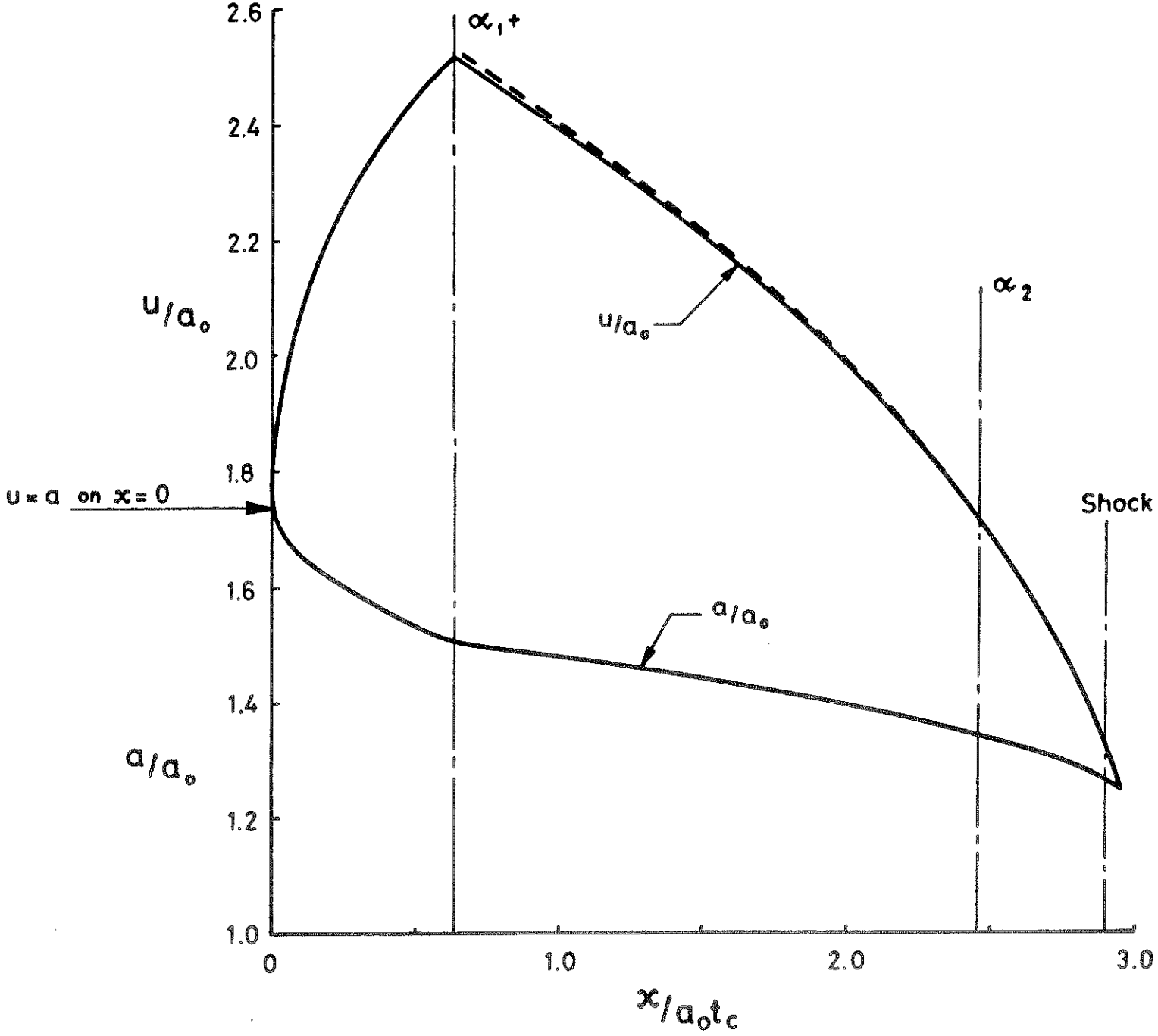
2.6
2.4
2.2
2.0
1.8
1.6
1.4
1.2
1.0
u/a_o
a/a_o
α_1+
α_2
u/a_o
a/a_o
u = a on x = 0
Shock
0
1.0
2.0
3.0
$x/a_o t_c$

Fig. 7.

Appendix A. Shape of the α- Characteristics

Defining y & z via

$$y^2 = (t + t_{sh})^2 - 4x t_{sh} a_0^{-1} \quad , \tag{A.1}$$

$$z = \left(\frac{3-\gamma}{\gamma+1}\right)\left\{ t + \left(\frac{\gamma+3}{\gamma-1}\right) t_{sh} \right\} \quad , \tag{A.2}$$

(5.3) in the text is equivalent to

$$yy' + y = Cz \quad , \quad C \equiv 2\frac{(\gamma^2-1)}{(3-\gamma)^2} \quad , \tag{A.3}$$

where y' is written for dy/dz. Defining

$$Y \equiv y' \quad , \tag{A.4}$$

rewriting (a.3a) in the form

$$y = \frac{Cz}{Y+1} \quad , \tag{A.5}$$

and differentiating (A.5) with respect to z gives the following separable differential equation for Y,

$$C\frac{dY}{d\zeta} = (Y+1)\left[C - Y(Y+1)\right] \quad , \zeta \equiv \ln z \, . \tag{A.6}$$

The solution of (A.6) is

$$\frac{Y+1}{\sqrt{Y^2+Y-C}} \left\{ \frac{1+2Y-\sqrt{1+4C}}{1+2Y+\sqrt{1+4C}} \right\}^{1/\left[2\sqrt{1+4C}\right]} = \frac{z}{K(\alpha)} \quad , \tag{A.7}$$

where $K(\alpha)$ is a constant that fixes the particular α-line whose shape is now given in parametric form, with Y as parameter, by (A.5 and 7), coupled with (A.1 and 2) of course.

General conclusions about α-line shape are hard to draw from this parametric form of the solution, but it is perfectly straightforward to choose a specific value for γ and proceed numerically. The α_1 and α_2 lines (Fig. 2) for $\gamma = 7/5$ are calculated in this way and are depicted in Fig. A.1.

Appendix B The Field Between $x=0$ and $x = x_1 +$

The required solution can be found by using the methods described by von Mises in Article 12 of his book (1958). The only novelty arises from the need here to treat a boundary-value problem, as opposed to the ones specifically described which analyse cases for which either initial or characteristic data are given. A brief account of salient features of the solution follows.

Equations (2.7 and 13) can be re-written in the forms

$$u_t + uu_x + av_x = 0 \quad , \quad v_t + uv_x + au_x = \bar{G} \quad . \qquad \text{B.1}$$

Since $\bar{G}$ vanishes in $x > 0$, transformation to the "speedgraph" plane (von Mises, 1958, page 162) leads to the pair of exact but linear homogeneous equations,

$$at_v - ut_u + x_u = 0 \quad , \quad at_u - ut_v + x_v = 0 \quad . \qquad \text{B.2}$$

Defining a potential V so that

$$x - ut = V_u \quad , \quad -at = V_v \quad , \qquad \text{B.3}$$

it can be shown from (B2) that V satisfies the linear second-order equation

$$V_{vv} - V_{uu} = -\left(\frac{3-\gamma}{\gamma-1}\right)\frac{1}{v}V_v \quad . \qquad \text{B.4}$$

The numerical coefficient on the right-hand side of (B.4) takes the value 4 if $\gamma = 7/5$. Restricting further work to this value of γ the general solution of (B.4) is

$$V = V(u,v) = v^{-3}\{f(\xi)+g(\eta)\} - v^{-2}\{f'(\xi)+g'(\eta)\} \quad , \qquad \text{B.5}$$

where

$$\xi = v + u \quad , \quad \eta = v - u \quad , \qquad \text{B.6}$$

and $(\,)'$ indicates differentiation with respect to the argument of the function.

Boundary-value information in the physical plane is given by

$$u = a = \tfrac{1}{2}(\gamma-1)v = \tfrac{1}{5}v \quad , \quad x = 0 \, , \, t \geq t_e \quad . \qquad \text{B.7}$$

The solutions in (6.9) show that when $u = a$ these velocities must both have the value

$$\left(\frac{2}{\gamma+1}\right)a_0 + \frac{4(\gamma-1)}{(3-\gamma)(\gamma+1)}a_0\frac{t}{t_c} = \frac{5}{12}\left(2+\frac{t}{t_c}\right)a_0 \qquad \text{B.8}$$

when γ is $7/5$. These statements translate into

$$V_u = -ut \quad , \quad V_v = -\tfrac{1}{5}vt \quad , \qquad \text{B.9}$$

when

$$\xi = \tfrac{5}{2}\left(2+\frac{t}{t_c}\right)a_0 \quad , \quad \eta = \tfrac{5}{3}\left(2+\frac{t}{t_c}\right)a_0 \, ,$$

in the speedgraph u,v plane. Use of (B.9) or (B.5) shows, after some rather tedious algebra, that

$$f(\xi) = f_5\xi^5 + f_6\xi^6 \quad ; \quad g(\eta) = g_5\eta^5 + g_6\eta^6 \quad , \qquad \text{B.10}$$

where

$$f_5 = -\frac{1}{40}t_c = g_5 \quad ;$$

$$f_6 = \frac{1691}{615600}\frac{t_c}{a_0} \quad ; \quad g_6 = \frac{21}{6400}\frac{t_c}{a_0} \, . \qquad \text{B.11}$$

The solution for gas velocity u and sound speed $a = \frac{1}{5}v$ as a function of x & t in the domain between $x = 0$ and $x = x_1 +$ is therefore given in the implicit form

$$(x-ut)v^3 = -5f_5\xi^3(\xi+2\eta) + 5g_5\eta^3(2\xi+\eta) - 3f_6\xi^4(3\xi+5\eta) + 3g_6\eta^4(5\xi+3\eta) \, , \qquad \text{B.12}$$

$$2v^5t = 5f_5\xi^3(\xi^2+5\xi\eta+10\eta^2) + 5g_5\eta^3(10\xi^2+5\xi\eta+\eta^2) + 5f_6\xi^4(3\xi^2+12\xi\eta+15\eta^2) + 5g_6\eta^4(15\xi^2+12\xi\eta+3\eta^2) \, . \qquad \text{B.13}$$

In order to find u as a function of x at a fixed t one can start by selecting values of η in the range $5a_0 \le \eta \le \frac{5}{3}(2+t/t_c)a_0$ and first solving (B.13) to find the corresponding ξ; the secant method for finding the roots of an equation is most effective here. The value of x at the chosen value of t then follows from (B.12) for each pair of associated ξ & η values, as do the values of u & v of course (see (B.6)).